Universality between Experiment and Simulation of a Diblock Copolymer Melt

Thomas M. Beardsley and Mark W. Matsen*
Department of Chemical Engineering, Department of Physics & Astronomy, and Waterloo Institute for Nanotechnology, University of Waterloo, Waterloo, Ontario, Canada N2L 3G1
(Received 18 September 2016; published 16 November 2016)

The equivalent behavior among analogous block copolymer systems involving chemically distinct molecules or mathematically different models has long hinted at an underlying universality, but only recently has it been rigorously demonstrated by matching results from different simulations. The profound implication of universality is that simple coarse-grained models can be calibrated so as to provide quantitatively accurate predictions to experiment. Here, we provide the first compelling demonstration of this by simulating a polyisoprene-polylactide diblock copolymer melt using a previously calibrated lattice model. The simulation successfully predicts the peak in the disordered-state structure function, the position of the order-disorder transition, and the latent heat of the transition in excellent quantitative agreement with experiment. This could mark a new era of precision in the field of block copolymer research.

DOI: 10.1103/PhysRevLett.117.217801

Block copolymers comprise a diverse family of self-assembling structured polymers with an ever-growing range of applications [1–5]. The testing ground for our understanding of their behavior is the simple linear AB diblock architecture, consisting of N_A A-type segments of statistical length a_A joined to N_B B-type segments of statistical length a_B (segments are defined to have a common volume of ρ_0^{-1}). Most of the theoretical work on these molecules is based on the standard Gaussian-chain model [6], where the incompatibility of the A and B segments is controlled by a phenomenological Flory-Huggins interaction parameter, χ. In mean-field theory, the tendency for the A and B blocks to segregate into ordered morphologies is controlled by the product χN and the geometry of the morphology is controlled by the composition $f_A \equiv N_A/N$, where $N \equiv N_A + N_B$. The ratio of the segment lengths, a_A/a_B, has a relatively minor effect on the behavior.

Fredrickson and Helfand (FH) [7] long ago predicted that the corrections to mean-field theory are controlled by the invariant polymerization index $\bar{N} = a^6\rho_0^2 N$, where $a = [f_A a_A^2 + (1-f_A)a_B^2]^{1/2}$ is the average segment length. The implication is that high molecular-weight diblocks exhibit universal behavior when expressed in terms of χN, f_A, a_A/a_B, and $\bar{N}$. In particular, the FH theory predicts that symmetric diblocks (i.e., $f_A = 0.5$ and $a_A = a_B$) transform from a disordered phase to a lamellar morphology at $(\chi N)_{\mathrm{ODT}} = 10.495 + 41.0\bar{N}^{-1/3}$. The relevant system parameters all have clear unambiguous definitions, apart from χ. Common practice is to approximate the interaction parameter by

$$\chi(T) = \frac{A}{T} + B, \tag{1}$$

where the fitting parameters A and B are adjusted so that the experimental order-disorder transition (ODT) or structure function $S(q)$ from small-angle scattering matches the predictions from FH [8]. When expressed in terms of the relevant parameters, experiments on chemically different diblock copolymers do indeed appear reasonably universal in that their phase diagrams are all qualitatively similar [9]. The same is true of simulations involving different models [10–14]. However, no one has seriously claimed that the universality among experiments and simulations is quantitatively precise, that is until recently.

Morse and co-workers have, in fact, suggested that the universality becomes mathematically exact for sufficiently large molecules. Focusing on the symmetric diblock, they have gone on to provide compelling evidence for this profound hypothesis. Their first major advance was a rigorous renormalized one-loop (ROL) calculation for $S(q)$ [15], which confirmed the long-held belief that the $\bar{N} \to \infty$ limit corresponds to mean-field theory. Shortly after, they accurately matched $S(q)$ from different simulation models, supporting the notion of universality [16]. Their most recent accomplishment was a method of defining χ by matching the peak of the structure function $S(q^*)$ to that of ROL [17]. With this definition, they successfully collapsed the ODTs from five different simulation models onto a single master curve given by the empirical relation,

$$(\chi N)_{\mathrm{ODT}} = 10.495 + 41.0\bar{N}^{-1/3} + 123.0\bar{N}^{-0.56}. \tag{2}$$

It is a testament to universality that this was accomplished with a wide selection of models including one involving hard-core interactions between the monomers, several more coarse-grained models with soft interactions, as well as the simple lattice model that we will be using in the current study. To date, the universality has been demonstrated for a range of other quantities: the free energy, the latent heat of

the transition, and the period, composition profile, and compressibility of the ordered lamellar phase [18].

Our aim is to demonstrate the true significance of universality, which is that experimental results can be accurately predicted using simple coarse-grained models. Gillard *et al.* [19] recently attempted such a demonstration, but with limited success. They focused on a polyisoprene-polylactide (PI-PLA) diblock copolymer with an ODT of $T_{\mathrm{ODT}} = 96 \pm 1\,^{\circ}\mathrm{C}$. The molecule was of composition $f_{\mathrm{PLA}} = 0.51$ and polymerization $N = 39$ (based on $\rho_0^{-1} = 118$ Å^3). The literature values for its segment lengths are $a_{\mathrm{PI}} = 6.1$ and $a_{\mathrm{PLA}} = 7.0$ Å, but Gillard *et al.* had to scale them up to $a_{\mathrm{PI}} = 7.2$ and $a_{\mathrm{PLA}} = 8.3$ Å in order to fit the peak heights $S(q^*)$ and peak positions q^* of the experimental scattering patterns to ROL, which in turn increased $\bar{N}$ from 231 to 611. The resulting fit gave $A = 381$ and $B = -0.48$ for the coefficients of $\chi(T)$, implying that $(\chi N)_{\mathrm{ODT}} = 21.8 \pm 0.1$, which is about 15% higher than the 18.7 predicted by Eq. (2). The simulations also predicted the latent heat of the transition to be $(\Delta H)_{\mathrm{ODT}} = 0.36$ J/g, which is 40% higher than the measured value of 0.26 ± 0.02 J/g [20].

Although the comparison is reasonable, it is not at the level one would expect if the universality is actually exact. It is also difficult to justify the ~20% increase in the segment lengths. The authors noted and later demonstrated [21] that polydispersity could be a contributing factor to the disagreement, given that the experimental molecules had a polydispersity index of $Đ = 1.10$, while Eq. (2) and the ROL used to calibrate $\chi(T)$ both assume monodisperse molecules. It is indeed well understood from mean-field theory [22–24] and Monte Carlo simulations [25] that polydispersity causes a significant increase in domain size and thus shifts the peak in $S(q)$ to lower q (see Supplemental Material [26]).

Here, we account for the effects of polydispersity by performing simulations on polydisperse molecules using the exact same lattice model as in Ref. [17]. The simulations are done in the canonical ensemble with a fixed number of polymers, n, each modeled as a sequence of beads (or monomers) connected by bonds of length b. The numbers of monomers in the γ blocks of a molecule ($\gamma = A$ and B) are given by independent Schulz-Zimm distributions [27,28] with number-average polymerizations of $(N_\gamma)_n$ and polydispersity indexes of $Đ_\gamma \equiv (N_\gamma)_w/(N_\gamma)_n$ (see Supplemental Material [26]). For polydisperse polymers, we define $N \equiv (N_A)_n + (N_B)_n$ and $f_A \equiv (N_A)_n/N$. To simplify the simulation, the monomers are restricted to a periodic fcc lattice with a maximum of one monomer per lattice site and bonded monomers occupying nearest-neighbor sites. Note that the nearest-neighbor spacing is set to $b = 2^{1/6} = 1.122$, such that the volume of the system V equals the total number of lattice sites. To allow room for the polymers to move, the lattice is only filled to a monomer density of $\rho_0 \equiv nN/V = 0.8$. Molecular interactions are limited to neighboring A and B monomers with an interaction strength of ϵ_{AB}. The simulations are performed by applying the standard Metropolis algorithm using three types of Monte Carlo moves, slithering snake, chain reversal, and crankshaft, with relative frequencies of 7:1:2 (see Ref. [29] for further details).

Our model has already been fully calibrated in Ref. [17]. From that, we know that its statistical segment length is given by $a = 1.233b = 1.384$, which implies $\bar{N} = 4.506N$. Furthermore, the previous study showed that the interaction parameter is well approximated by

$$\chi(\alpha) = \frac{z_\infty \alpha + c_1 \alpha^2}{1 + c_2 \alpha}, \tag{3}$$

where $\alpha \equiv \epsilon_{AB}/k_B T$ and $z_\infty = 4.897$ is the average number of intermolecular contacts a monomer experiences in the limit $\alpha = 0$ and $N \to \infty$. The fitting parameters, $c_1 = 88.5$ and $c_2 = 8.30$, were obtained in Ref. [17] by matching curves of $S(q^*)$ vs χN from monodisperse simulations to ROL across the entire disordered phase for seven different chain lengths ranging from $N = 20$ to 180. For the current simulations, we represent the PI-PLA diblock by setting $(N_A)_n = (N_B)_n = 25$ and $Đ_A = Đ_B = 1.2$, which gives $f_A = 0.5$, $\bar{N} = 225$ and $Đ = 1.1$ [30]. All our simulations are performed in a cubic simulation box of volume $V = 171500$, containing $n = 2744$ molecules.

In order to calibrate the experimental interaction parameter $\chi(T)$ we first need to simulate the disordered-state structure function,

$$S(\mathbf{q}) = \frac{1}{4V}\left\langle \left| \sum_{j=1}^{V} \sigma_j \exp(i\mathbf{q}\cdot\mathbf{r}_j) \right|^2 \right\rangle, \tag{4}$$

where angle brackets denote ensemble average, $\mathbf{r}_j$ is the position of the jth lattice site, and $\sigma_j = 1, 0$ or -1 if the site is occupied by an A monomer, a vacancy or a B monomer, respectively. Results are plotted in Fig. 1 for several different interaction strengths in the disordered phase. To illustrate the effect of polydispersity, $S(q)$ is simulated for both monodisperse and polydisperse diblocks. Because of the finite size of our simulation box, $S(q)$ is only defined for a discrete set of wave vectors, $\mathbf{q}$. To accurately extract the peak position q^* and peak height $S(q^*)$ we fit our simulation data to the RPA structure function [23–25] (see Supplemental Material [26]).

The peak heights $S(q^*)$ for monodisperse (squares) and polydisperse (circles) diblocks are plotted in Fig. 2 as a function of χN using Eq. (3). Because our model is already calibrated, the monodisperse results match the ROL prediction, which Gillard *et al.* [19] used to determine $\chi(T)$ for the experimental system. Here, we instead fit the experimental results (crosses) to our polydisperse simulation, which gives $A = 534$ and $B = -0.82$. Polydispersity clearly has a sizable effect on $S(q^*)$, and thus our analysis

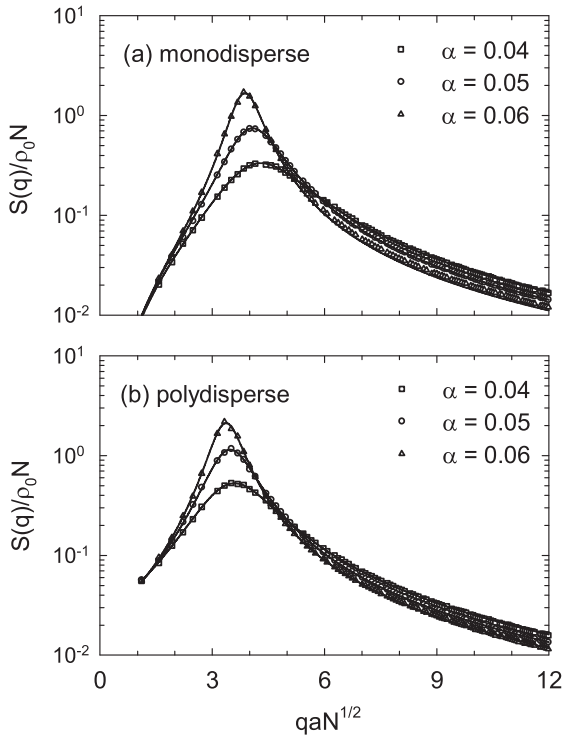

FIG. 1. Disordered-state structure function $S(q)$, calculated for (a) monodisperse and (b) polydisperse melts at different values of $\alpha = \epsilon_{AB}/k_BT$. The solid curves are fits using the RPA structure function.

provides a far more accurate estimation of $\chi(T)$. With our improved calibration, the experimental ODT now maps to $(\chi N)_{\mathrm{ODT}} = 24.5 \pm 0.2$.

To check the consistency of our simulations with the experiment, Fig. 3 compares the peak position q^* of the structure function. For the experiment, the peak is scaled with respect to the average segment length, $a = 6.6$ Å, obtained from the literature values of a_{PI} and a_{PLA}. It is

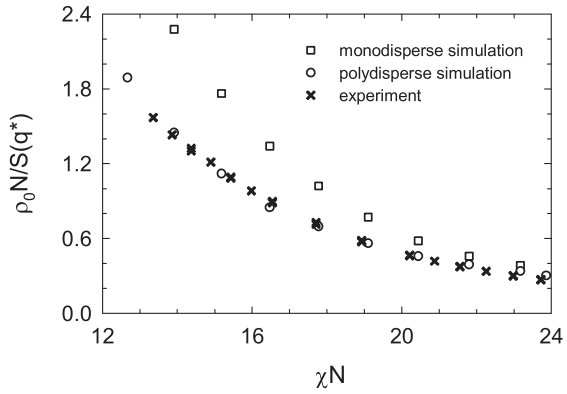

FIG. 2. Peak in the disordered-state structure function $S(q^*)$ from simulations of monodisperse (squares) and polydisperse (circles) diblock copolymers compared to that of the experiment (crosses). Experimental results are plotted using $A = 534$ and $B = -0.82$ for $\chi(T)$.

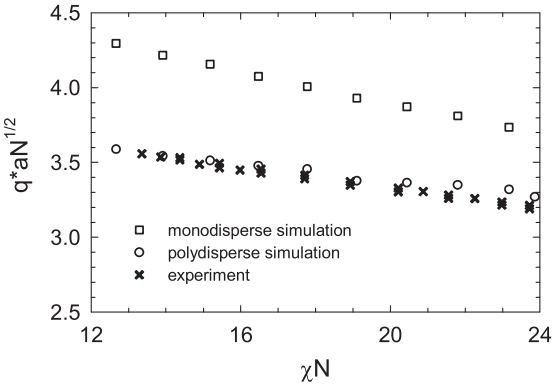

FIG. 3. Peak position q^* of the disordered-state structure function $S(q)$ from simulations of monodisperse (squares) and polydisperse (circles) diblock copolymers compared to that of the experiment (crosses). Experimental results are plotted using $a = 6.6$ Å.

clear that the experimental results are completely consistent with the polydisperse simulation (circles), whereas the results for the monodisperse simulation (squares) are 16%–22% larger. This is the approximate factor by which Gillard *et al.* had to increase the literature value of a, leading them to assume $\bar{N} = 611$ instead of 231. Evidently, the factor was simply compensating for the fact that the ROL prediction used in their analysis was specific to monodisperse polymers.

Equation (2) predicts $(\chi N)_{\mathrm{ODT}} = 23.0$ for $\bar{N} = 231$, but this again assumes monodisperse polymers. To account for polydispersity, we locate the ODT by simulation. This is done by evaluating the average number of A-B contacts, $\langle n_{AB} \rangle$, as a function of χN using parallel tempering [13]. To gauge the level of metastability, Fig. 4 plots results from two separate simulations. The first (circles) initialized the system with a configuration equilibrated in the disordered

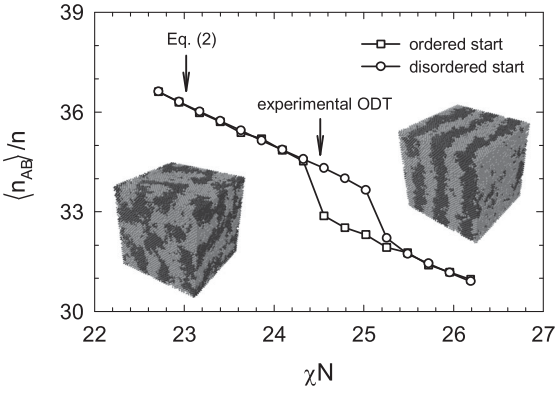

FIG. 4. Average number of A-B contacts, $\langle n_{AB} \rangle$, as a function of the interaction parameter $\chi(\alpha)$ from parallel tempering runs initialized with disordered (circles) and lamellar (squares) configurations shown by the insets. The arrows denote the experimental ODT and the prediction from Eq. (2) for monodisperse polymers.

phase. At the higher values of χN, the system spontaneously orders into (300) and (221) lamellar phases, resulting in a discontinuous reduction in $\langle n_{AB}\rangle$. The principle wave vectors of the (300) and (221) orientations have the same magnitude, which, as expected, matches the peak in $S(q)$ at the ODT. Our second simulation (squares) was initialized from one of the (300) configurations; another simulation (not shown) initialized with a (221) configuration gave equivalent results. Comparing the two simulations in Fig. 4 reveals a narrow metastability interval, where the lifetimes of the disordered and ordered phases exceed our simulation time. From this, we conclude that $(\chi N)_{\mathrm{ODT}} = 24.8 \pm 0.3$, which nicely overlaps the experimental result, 24.5 ± 0.2. Incidentally, Arora *et al.* [31] have shown that the actual ODT from simulation tends to be at the low-χN end of the metastability interval, which agrees precisely with the experimental ODT.

The jump in the number of A-B contacts, $\Delta\langle n_{AB}\rangle$, in Fig. 4 at the ODT is related to the latent heat of the transition by [19]

$$(\Delta H)_{\mathrm{ODT}} = \frac{\Delta\langle n_{\mathrm{AB}}\rangle}{n}\frac{RA}{\chi'(\alpha_{\mathrm{ODT}})M_n}, \tag{5}$$

where R is the ideal gas constant and $M_n = 2750$ g/mol is the number-average molar mass of the diblock copolymer. Inserting $\Delta\langle n_{AB}\rangle/n = 1.44$ from our simulation gives $(\Delta H)_{\mathrm{ODT}} = 0.277$ J/g, which agrees with the experiment to within the reported uncertainty [20].

There are several sources of inaccuracy in our simulation of the PI-PLA diblock copolymer melt. For instance, the limitations of the lattice model prevent us from accounting for the conformational asymmetry (i.e., $a_{\mathrm{PLA}}/a_{\mathrm{PI}} = 1.15$). Nevertheless, this asymmetry has little effect on $S(q)$ and the ODT in mean-field theory (see Supplemental Material [26]), and this presumably remains the same when fluctuations are included. There is also the issue that we had to assume $Đ_A = Đ_B$, since the experiment only measured the overall polydispersity

$$Đ = f_A^2(Đ_A - 1) + (1 - f_A)^2(Đ_B - 1) + 1. \tag{6}$$

Likewise, mean-field theory predicts that changing the balance of polydispersity among the two blocks has little effect on $S(q)$ (see Supplemental Material [26]). Of course, the actual molecular-weight distribution will differ somewhat from the Schulz-Zimm distribution, but we know that the shape of the distribution has a negligible effect when Đ is small [24,32]. Thus, the inaccuracies in our simulation due to conformational asymmetry and the unknown details of the polydispersity distribution should be relatively small.

The present agreement between experiment and simulation cements the compelling evidence for the universality hypothesis previously obtained by matching results from different simulation models [17,18]. The significance of this universality cannot be overstated. Without universality, a detailed microscopic model would be required to obtain quantitatively accurate predictions, but with the universality, even our simple lattice model is sufficient. One just needs to determine the relevant system parameters (e.g., χ, N, f, a_A, a_B, $Đ_A$ and $Đ_B$). Apart from χ, all the parameters are well defined for both experiment and simulation.

In principle, the particular experiment and simulation of our study can be matched without referring to χ. We could simply fit the experiment to our model by matching $S(q^*)$ vs T, assuming a nonlinear functional form for $\alpha(T)$ with several fitting parameters. However, the universality applies to all systems and so it is best to choose a more general reference, the Flory-Huggins χ parameter. To do this, we should fit experiments and simulations to the most accurate theoretical prediction for the standard Gaussian-chain model, and at the moment this is undoubtedly the ROL prediction for $S(q)$, which becomes exact as $\bar{N} \to \infty$.

Naturally, the universality will become inaccurate as $\bar{N}$ decreases. Nevertheless, our demonstration worked for a remarkably small value of $\bar{N} = 231$, as was the case in Ref. [17] where the ODTs of the different simulations were matched down to $\bar{N} \approx 200$. This begs the question of just how far does the universality extend. It will most certainly depend upon the details of the specific system. For instance, the universality is certain to breakdown once the polymers are short relative to their persistence length or once the range of the interactions is no longer small relative to the size of the molecules. We will have to wait for future studies to see just how widely applicable the universality is, but all indications are that it will be valid for most experimental systems.

An important result from our study is the accurate prediction of $\chi(T)$ for PI-PLA interactions, which gives $\chi = 0.627$ at $T_{\mathrm{ODT}} = 96\,°\mathrm{C}$ as compared to the previous estimations of 0.227 [33] and 0.552 [19]. Although our prediction will be affected by statistical inaccuracy in the simulation of $S(q)$, this is well controlled and relatively minor. A more significant source of inaccuracy is the experimental measurement of $S(q)$, given the involved process required to obtain absolute scattering intensities [19]. However, the largest source is likely from the characterization of the PI-PLA diblock copolymer, in particular the 5% uncertainty in $N = 39$ [19]. Even if we can determine values of χN accurately, any uncertainty in N will necessarily limit the accuracy of $\chi(T)$ by a similar degree. Still, our estimate of $\chi(T)$ is undoubtedly the most accurate to date performed for any pair of chemical species. The improved method of defining $\chi(T)$ demonstrated in our study coupled with precision experiments and synthesis will hopefully lead to a new level of accuracy in determining $\chi(T)$ for other chemical pairs. With the added precision, researchers will be well equipped to investigate subtle effects in block copolymer materials using a combination of theory, simulation, and experiment.

In conclusion, we have shown that the accurate universality recently demonstrated among different simulation models for diblock copolymer melts [17,18] also extends to experiments. By matching the peak in the experimental structure function $S(q^*)$ of a PI-PLA diblock copolymer melt [19,20] with that of a calibrated simulation model [17], we provide what is undoubtedly the most accurate estimation of $\chi(T)$ for a pair of chemical species (i.e., PI and PLA). This allowed us to directly compare the ODT of the experiment with a Monte Carlo simulation in terms of χN. The position of the ODT as well as the latent heat of the transition quantitatively agree to within the small experimental uncertainties and statistical inaccuracies. This unprecedented agreement is likely to usher in a new era of precision between experiment, simulation, and theory. The key to achieving it was accounting for the modest polydispersity in the experimental system (i.e., $Đ = 1.10$), emphasizing that researchers may have to start considering effects that have gone largely ignored in the past.

We are grateful to Dave Morse, Tim Gillard, and Frank Bates for valuable discussions and for providing us with their experimental data. This work was funded by NSF under the Center for Sustainable Polymers (CHE-1413862), and computer resources were provided by SHARCNET of Compute Canada.

*mwmatsen@uwaterloo.ca

[1] F. S. Bates and G. H. Fredrickson, Phys. Today **52**, 32 (1999).
[2] T. P. Lodge, Macromol. Chem. Phys. **204**, 265 (2003).
[3] A.-V. Ruzette and L. Leibler, Nat. Mater. **4**, 19 (2005).
[4] F. S. Bates, M. A. Hillmyer, T. P. Lodge, C. M. Bates, K. T. Delaney, and G. H. Fredrickson, Science **336**, 434 (2012).
[5] Y. Mai and A. Eisenberg, Chem. Soc. Rev. **41**, 5969 (2012).
[6] M. W. Matsen, J. Phys. Condens. Matter **14**, R21 (2002).
[7] G. H. Fredrickson and E. Helfand, J. Chem. Phys. **87**, 697 (1987).
[8] W. W. Maurer, F. S. Bates, T. P. Lodge, K. Almdal, K. Mortensen, and G. H. Fredrickson, J. Chem. Phys. **108**, 2989 (1998).
[9] F. S. Bates, M. F. Schulz, A. K. Khandpur, S. Föster, J. H. Rosedale, K. Almdal, and K. Mortensen, Faraday Discuss. **98**, 7 (1994).
[10] A. J. Schultz, C. K. Hall, and J. Genzer, J. Chem. Phys. **117**, 10329 (2002).
[11] F. J. Martinez-Veracoechea and F. A. Escobedo, J. Chem. Phys. **125**, 104907 (2006).
[12] E. M Lennon, K. Katsov, and G. H. Fredrickson, Phys. Rev. Lett. **101**, 138302 (2008).
[13] T. M. Beardsley and M. W. Matsen, Eur. Phys. J. E **32**, 255 (2010).
[14] J. H. Ryu, H. S. Wee, and W. B. Lee, Phys. Rev. E **94**, 032501 (2016).
[15] J. Qin and D. C. Morse, Phys. Rev. Lett. **108**, 238301 (2012).
[16] J. Glaser, J. Qin, P. Medapuram, M. Müller, and D. C. Morse, Soft Matter **8**, 11310 (2012).
[17] J. Glaser, P. Medapuram, T. M. Beardsley, M. W. Matsen, and D. C. Morse, Phys. Rev. Lett. **113**, 068302 (2014).
[18] P. Medapuram, J. Glaser, and D. C. Morse, Macromolecules **48**, 819 (2015).
[19] T. G. Gillard, P. Medapuram, D. C. Morse, and F. S. Bates, Macromolecules **48**, 2801 (2015).
[20] T. G. Gillard, D. Phelan, C. Leighton, and F. S. Bates, Macromolecules **48**, 4733 (2015).
[21] P. Medapuram, Ph.D. thesis, University of Minnesota, 2016.
[22] M. W. Matsen, Eur. Phys. J. E **21**, 199 (2006).
[23] S. W. Sides and G. H. Fredrickson, J. Chem. Phys. **121**, 4974 (2004).
[24] D. M. Cooke and A.-C. Shi, Macromolecules **39**, 6661 (2006).
[25] T. M. Beardsley and M. W. Matsen, Eur. Phys. J. E **27**, 323 (2008).
[26] See Supplemental Material at http://link.aps.org/supplemental/10.1103/PhysRevLett.117.217801 for the behavior of the RPA structure function, $S_{\mathrm{RPA}}(q)$, for polydisperse diblock copolymer melts.
[27] G. V. Schulz, Z. Phys. Chem. (Munich) **B43**, 25 (1939).
[28] B. H. Zimm, J. Chem. Phys. **16**, 1099 (1948).
[29] O. N. Vassiliev and M. W. Matsen, J. Chem. Phys. **118**, 7700 (2003).
[30] The individual values of χ and N from the experiment and simulation do not match because different reference volumes, ρ_0^{-1}, are used to define the segments.
[31] A. Arora, D. C. Morse, F. S. Bates, and K. D. Dorfman, Soft Matter **11**, 4862 (2015).
[32] N. A. Lynd, M. A. Hillmyer, and M. W. Matsen, Macromolecules **41**, 4531 (2008).
[33] S. Lee, T. M. Gillard, and F. S. Bates, AIChE J. **59**, 3502 (2013); the χ values in this paper are based on a slightly different reference volume of $\rho_0^{-1} = 110$ Å.

Universality between Experiment and Simulation of a Diblock Copolymer Melt: Supplemental Material

Thomas M. Beardsley and Mark W. Matsen*
Department of Chemical Engineering, Department of Physics & Astronomy, and Waterloo Institute for Nanotechnology, University of Waterloo, Waterloo, Ontario, Canada

Due to a lack of information, certain assumptions had to be made about the polydispersity of the PI-PLA diblock copolymer used in the experiments [1, 2]. Since the molecule was created using a two-step synthesis, the molecular-weight distributions of the two blocks should be independent. For each block, we employ the usual Schulz-Zimm distribution [3, 4]

$$p(N_\gamma) = \frac{k_\gamma^{k_\gamma} N_\gamma^{k_\gamma-1}}{(N_\gamma)_n^{k_\gamma}\Gamma(k_\gamma)} \exp\left(-\frac{k_\gamma N_\gamma}{(N_\gamma)_n}\right) , \qquad (1)$$

where $Đ_\gamma \equiv (N_\gamma)_w/(N_\gamma)_n = 1 + 1/k_\gamma$ (γ = A or B). The Schulz-Zimm distribution assumes N_γ is a continuous variable whereas it is restricted to integer values in our simulation, and therefore we approximate the distribution using a procedure devised in Ref. [5]. Because the experiments only provide the polydispersity index of the entire molecule (*i.e.*, $Đ = 1.10$), we assume the two blocks have equal polydispersities of $Đ_A = Đ_B = 1.2$. As illustrated in Fig. 1, this polydispersity index corresponds to a broad molecular-weight distribution, and thus it is not surprising that the modest $Đ = 1.10$ by experimental standards can have a significant effect on results.

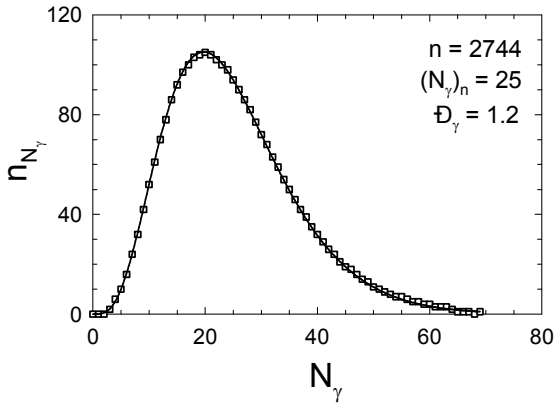

FIG. 1. Discrete distribution, $\{n_{N_\gamma}\}$, calculated for a system of $n = 2744$ molecules with a number-average polymerization of $(N_\gamma)_n = 25$ and polydispersity index of $Đ_\gamma = 1.2$. The solid curve compares $np(N_\gamma)$ from the continuous Schulz-Zimm distribution in Eq. (1).

To extract the peak of the disordered-state structure function from our simulations, we fit our data to the mean-field (or RPA) approximation using χN, $\rho_0 N$ and $aN^{1/2}$ as fitting parameters. The RPA structure function for the Schulz-Zimm distribution [6, 7] is given by

$$\frac{S_{\rm RPA}(q)}{\rho_0 N} = \frac{1}{F(q) - 2\chi N} , \qquad (2)$$

where

$$F(q) = \frac{S_{\rm AA} + S_{\rm BB} + 2S_{\rm AB}}{(S_{\rm AA}S_{\rm BB} - S_{\rm AB}^2)} , \qquad (3)$$

$$S_{\rm AA} = \frac{2f_{\rm A}^2}{x_{\rm A}^2}\left[\left(1+\frac{x_{\rm A}}{k_{\rm A}}\right)^{-k_{\rm A}} + x_{\rm A} - 1\right] , \qquad (4)$$

$$S_{\rm BB} = \frac{2(1-f_{\rm A})^2}{x_{\rm B}^2}\left[\left(1+\frac{x_{\rm B}}{k_{\rm B}}\right)^{-k_{\rm B}} + x_{\rm B} - 1\right] , \qquad (5)$$

$$S_{\rm AB} = \frac{f_{\rm A}(1-f_{\rm A})}{x_{\rm A}x_{\rm B}}\left[\left(1+\frac{x_{\rm A}}{k_{\rm A}}\right)^{-k_{\rm A}} - 1\right] \times \left[\left(1+\frac{x_{\rm B}}{k_{\rm B}}\right)^{-k_{\rm B}} - 1\right] , \qquad (6)$$

and $x_\gamma \equiv q^2 a_\gamma^2 (N_\gamma)_n/6$. The monodisperse limit is evaluated using

$$\lim_{k\to\infty}\left(1+\frac{x}{k}\right)^{-k} = \exp(-x) . \qquad (7)$$

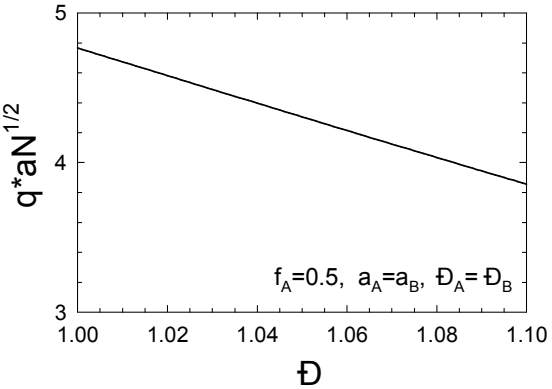

FIG. 2. Peak position, q^*, of the RPA structure function as a function of polydispersity, Đ, calculated for a symmetric diblock with $f_A = 0.5$, $a_A = a_B$ and $Đ_A = Đ_B$.

Given the form of Eq. (2), it follows that the peak in the RPA structure function, $S_{\rm RPA}(q^*)$, corresponds to the minimum in $F(q)$ irrespective of χN. The resulting peak position is plotted in Fig. 2 as a function of the

overall polydispersity, Đ, for a symmetric diblock copolymer. Although mean-field theory overestimates q^* by a considerable amount, it does capture the approximate 20% difference between the monodisperse and polydisperse simulations in Fig. 3 of our paper.

The RPA structure function can be used to gauge the effect of a mismatch in $Đ_A$ and $Đ_B$. Figure 3(a) shows that the peak position, q^*, varies by only 2.5% as the polydispersity changes from being equally split between the two blocks (*i.e.*, $Đ_A = 1.2$) to being entirely in one block (*i.e.*, $Đ_A = 1.0$ or 1.4). Furthermore, Fig. 3(b) shows that $F(q^*)$, which controls the peak height, varies by only 1.7%. Thus for any modest imbalance in the polydispersites, the effect on the mean-field $S_{\mathrm{RPA}}(q)$ will be tiny, and we can assume the same is true when fluctuations are included.

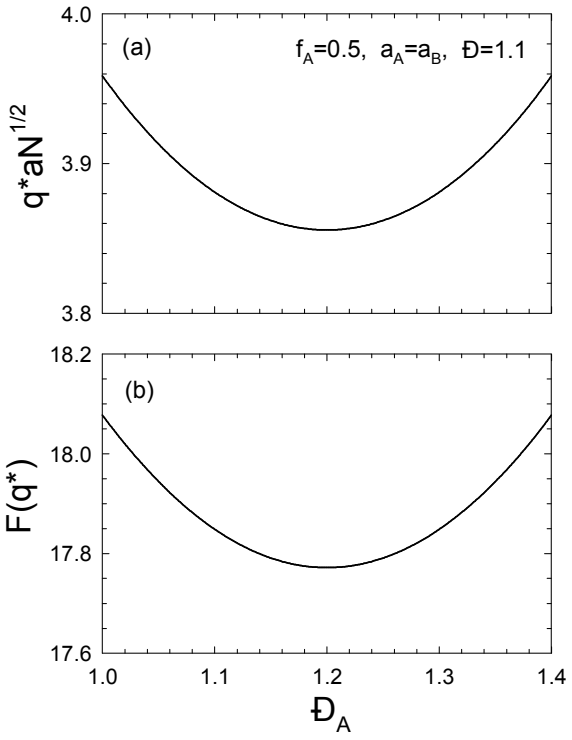

FIG. 3. Effect of polydispersity asymmetry on (a) the position of the peak, q^*, in the RPA structure function and (b) the quantity, $F(q^*)$, controlling the peak height.

Due to the nature of our lattice model, the simulations had to assume conformationally symmetric molecules (*i.e.*, $a_A/a_B = 1$), whereas the actual ratio of segment lengths in the experiment is 7.0Å/6.1Å $= 1.15$. Again, we can refer to $S_{\mathrm{RPA}}(q)$ to gauge the significance of this asymmetry. Figure 4 shows analogous plots to those of Fig. 3, but this time for a mismatch in a_A and a_B. The effect of the asymmetry is clearly negligible, thus justifying our approximation of conformational symmetry. Likewise, it is easy to demonstrate that the slight compositional asymmetry in the experiments (*i.e.*, $f_{\mathrm{PLA}} = 0.51$) should also have a negligible effect.

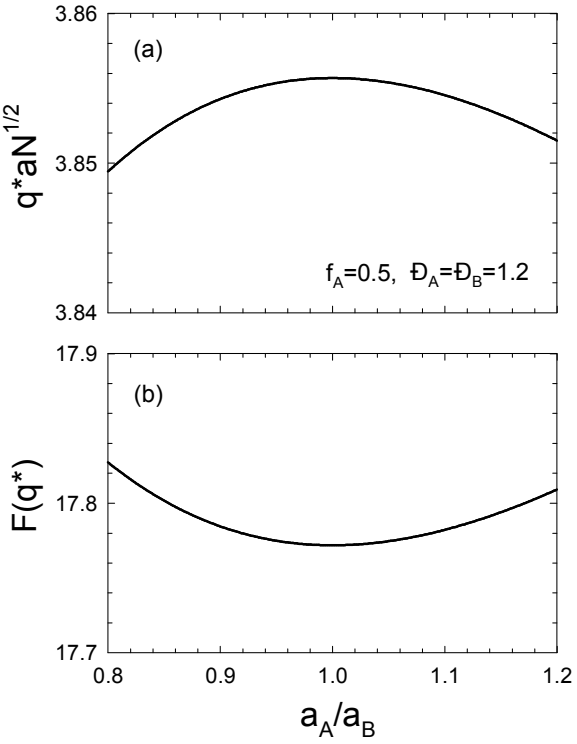

FIG. 4. Effect of conformational asymmetry on (a) the position of the peak, q^*, in the RPA structure function and (b) the quantity, $F(q^*)$, controlling the peak height.

* mwmatsen@uwaterloo.ca

[1] T. G. Gillard, P. Medapuram, D. C. Morse and F. S. Bates, Macromolecules **48** 2801 (2015).
[2] T. G. Gillard, D. Phelan, C. Leighton and F. S. Bates, Macromolecules **48** 4733 (2015).
[3] G. V. Schulz, Z. Phys. Chem. (Munich) **B43**, 25 (1939).
[4] B. H. Zimm, J. Chem. Phys. **16**, 1099 (1948).
[5] T. M. Beardsley and M. W. Matsen, Eur. Phys. J. E **27**, 323 (2008).
[6] S. W. Sides and G. H. Fredrickson, J. Chem. Phys. **121**, 4974 (2004).
[7] D. M. Cooke and A.-C. Shi, Macromolecules **39**, 6661 (2006).